# Analysis of Effect of Inclined Magnetic Field on MHD Boundary Layer Flow over a porous Exponentially Stretching Sheet subject to Thermal Radiation


## ABSTRACT

MHD flow has a wide range of industrial applications such as MHD propulsion for space exploration, cooling of nuclear reactors, electronic packages, microelectronic devices, and many more. Due to this, a study on the MHD boundary layer flow of a viscous incompressible fluid over an exponentially stretching sheet with an inclined magnetic field in presence of thermal radiation is analyzed. The continuity, momentum, and energy equations governing the fluid motion are obtained. They are then transformed into a system of nonlinear ordinary differential equations using suitable similarity transformation variables. The resulting nonlinear ordinary differential equations are then transformed to a system of first-order ordinary differential equations and the numerical solution is executed using the collocation method. The effects of the magnetic field, angle of inclination, radiation, Prandtl number, and the exponential stretching of the sheet on the velocity and temperature of the fluid are discussed. It is observed that velocity increases as the sheet is stretched and decreases as the magnetic field and angle of inclination of the magnetic field increases. Temperature increases as magnetic field, angle of inclination, and radiation increase and lowers as the stretching and stratification parameter of the sheet and Prandtl number increases. The findings of this study are in agreement with other previously related work done.



*Keywords: Inclined Magnetic field, Hydrodynamic boundary layer flow*


## 1. INTRODUCTION

The flow of fluids over a stretching sheet is considered a very important phenomenon to study due to its wide application in industrial processes such as in the production of polymer sheets, filaments, and wires. The assumption is that the stirring sheet move on its own plane and the stretched surface interacts with ambient fluid both impulsively and thermally. The presence of a magnetic field on the MHD boundary layer flow of a viscous incompressible fluid over an exponentially porous stretching sheet has some negative effects on the velocity of fluid flow. When the magnetic field is perpendicular to the stretching sheet the velocity of the fluid is suppressed. Suppression of the velocity of the fluid by the magnetic field can be controlled by inclining the magnetic field, which allows for the variation of the angle of inclination. This makes systems with the inclined magnetic field have the velocity of a fluid on them increased due to minimization of suppression. The concept of the boundary layer was brought by Ludwig Prandtl [1874-1953] in his paper of 1904. His work on the boundary layer formed the basis for future work on skin friction, heat transfer, and separation. Due to drag the fluid velocity immediately adjacent to the surface is zero and the fluid layer next to the surface becomes attracted to the surface. That is, wets the surface. This condition is known as the 'no-slip condition'.[1] investigated and discussed the effects of slip condition and Newtonian heating on MHD flow of Casson fluid over a non-linearly stretching sheet saturated in a porous medium. The analysis of MHD boundary layer flow and heat transfer towards a porous exponentially stretching sheet in presence of thermal radiation was studied by [2]. The effect of magnetic field on MHD convective

flow was investigated by [3] and [4], whereby they looked at mixed convective and steady free convective respectively. The idea of convection was extended by [5] where he incorporated thermal radiation and based his study on nanofluid flow. This work was also investigated by [6] but used the spectral relaxation method in his analysis. [7] Investigated the effect of viscosity and thermal conductivity on heat and mass transfer flow of nanofluid. Then the effect of suction/injection on MHD free-convection flow in a vertical channel with thermal radiation was discussed by [8]. [9] researched Newtonian heating and convective boundary conditions on MHD flow, whereby he considered a flow over a stretching sheet in presence of Joule heating. Heat transfer of third-grade fluid flow in a pipe under an externally applied magnetic field with convection on the wall was investigated by [10]. This work was extended by [11], whereby their study was based on Casson fluid over a moving vertical plate embedded in a porous medium. The work on MHD boundary layer flow of Darcy-Forchheimer convection in a nanofluid was also put into consideration by [12] and [13] continued this work by considering a flow past a wedge. The effect of magnetic fields on the boundary layer flow with variable viscosity in presence of thermal radiation was continued by [14]. [15] Extended this work by considering ferrofluid and convective boundary conditions. Effects of Newtonian heating on boundary layer flow of non-Newtonian MHD nanofluid was well discussed by [16] where spectral relaxation method was used. This area was also explored by [17].On thermal conductivity and radiation,[18–20] dealt with it conclusively. Then [21] extended their work on impacts of Newtonian heating, variable fluid properties, and Cattaneo-Christov model on MHD stagnation point flow of Walters'B fluid induced by stretching surface. Basing my argument on the recent researches done as described above, the field of MHD is not fully explored. This has resulted to the present work which involves the analysis of the effect of inclined magnetic field on MHD boundary layer flow over a porous exponentially stretching sheet subject to thermal radiation.

## 2. MATHEMATICAL FORMULATION

In this study a magnetic field, $B$ inclined at an angle $\alpha$ to the horizontal flat sheet and how it influences the flow is considered. To achieve this we consider the flow of an incompressible viscous fluid past a flat sheet coinciding with the plane y=0 in a densely saturated porous medium with a non–uniform permeability $k$

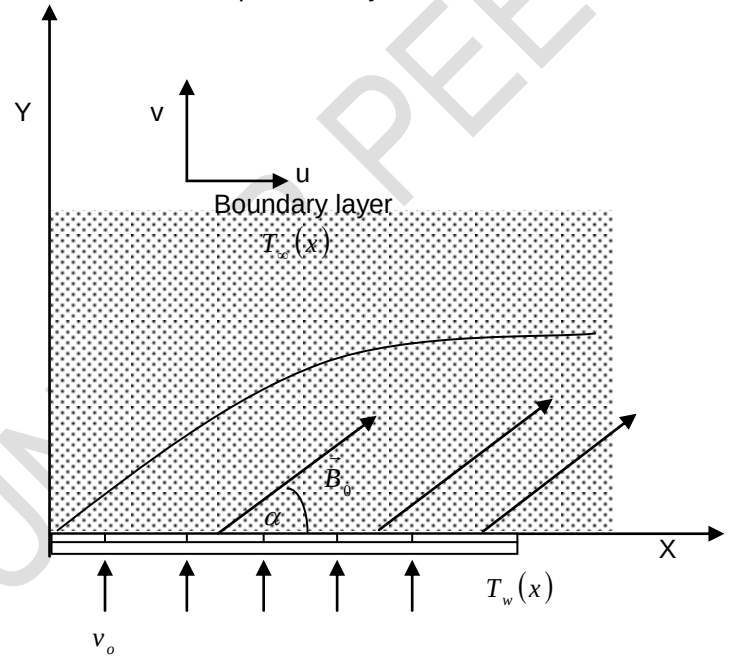


**Figure 1: Sketch of the physical problem.**

Assuming that the fluid flow is restricted to y>0, two equal and opposite forces are applied along the x-axis so that the wall is stretched keeping the origin fixed. These two equal and opposite forces cause asymmetric boundary at the centre of the porous medium (see fig 1). A variable

magnetic field $\vec{B}(x) = \vec{B}_0 e^{\frac{Nx}{2L}}$ is applied inclined at an angle $\alpha$ to the sheet where from figure 1, $\vec{B}_0$ which is a constant is expressed as $\vec{B}_0 = (B_0 \cos\alpha, B_0 \sin\alpha, 0)$. Then a two-dimensional steady flow in a magnetic field $\vec{B}$, induces an electric current density $\vec{J}$. The induced current creates forces on the liquid and changes the magnetic field. Each volume of the fluid having a magnetic field $\vec{B}$ experiences a Lorentz force given by $\vec{J} \times \vec{B} = -\sigma u B^2 \sin^2\alpha$.

Let the sheet of temperature $T_w(x)$ be embedded in a thermally stratified medium of variable ambient temperature $T_\infty(x)$, where $T_w(x) > T_\infty(x)$ .we define $T_w(x) = T_0 + be^{\frac{Nx}{2L}}$ and $T_\infty(x) = T_0 + ce^{\frac{Nx}{2L}}$ where $T_0$ is the reference temperature, $b > 0, c \geq 0$ are constants. The continuity, momentum and energy equations governing this flow are given by the equations below

$$\frac{\partial u}{\partial x} + \frac{\partial u}{\partial y} = 0 \tag{1}$$

$$u\frac{\partial u}{\partial x} + v\frac{\partial u}{\partial y} = \upsilon\frac{\partial^2 u}{\partial y^2} - \frac{\upsilon}{k}u - \sigma\frac{B^2 \sin^2\alpha}{\rho}u \tag{2}$$

$$u\frac{\partial T}{\partial x} + v\frac{\partial T}{\partial y} = \frac{\kappa}{\rho c_p}\frac{\partial^2 T}{\partial y^2} - \frac{1}{\rho c_p}\frac{16\sigma T_\infty^3}{3k^*}\frac{\partial^2 T}{\partial y^2} \tag{3}$$

The boundary conditions for the differential equations above are

$$u = U \quad , v = V(x) \quad , T = T_w(x) \quad \text{at } y = 0 \tag{4}$$

$$u \to 0, \quad T = T_\infty(x) \quad \text{as } y \to \infty \tag{5}$$

Where $u$ and $v$ are the components of velocity in the x and y direction respectively, $\upsilon = \frac{\mu}{\rho}$ is the kinematics viscosity, $\rho$ is the fluid density, $\mu$ is the coefficient of fluid viscosity, $c_p$ is the specific heat capacity at constant pressure, and $\kappa$ is the thermal conductivity of the fluid. $U = U_0 e^{\frac{Nx}{L}}$ Is the stretching velocity, $U_0$ is the reference velocity $V(x) < 0$ is the velocity of blowing and $V(x) = V_0 e^{\frac{Nx}{2L}}$, is a special type of velocity at the wall considered. $V_0$ is the initial strength of injection (blowing)

### 2.1 Similarity transformation

By introducing the similarity transformation variables

$$\eta = \sqrt{\frac{U_0}{2\upsilon L}}\, e^{\frac{Nx}{2L}} y \quad , \quad u = U_0 e^{\frac{Nx}{2L}}$$

$$v = -N\sqrt{\frac{\upsilon U_0}{2L}} e^{\frac{Nx}{2L}} \left( f(\eta) + \eta f'(\eta) \right) \quad , \quad \theta(\eta) = \frac{T - T_\infty}{T_w - T_0} \tag{6}$$

Using them in equations 2 and 3, we transform the governing equations as below
For equation 2

$$f''' - 2Nf'^2 + Nff'' - (k_1 + 2M^2 \sin^2 \alpha) f' = 0 \quad (7)$$

Where $k_1 = \frac{2\upsilon L}{k_0 U_0}$ and $M = B_0 \frac{\sqrt{L\sigma}}{\rho U_0}$

Then equation 3 reduces to

$$\{1 + \frac{4}{3} Rd\} \theta'' + N \Pr\{ f\theta' - \theta f'\} - N \Pr St f' = 0 \quad (8)$$

Where $\Pr = \frac{\mu c_p}{\kappa}$, $St = \frac{c}{b}$ and $Rd = \frac{4\sigma T_\infty^3}{k^* \kappa}$

The boundary conditions associated with these equations are transformed as below using the boundary conditions (4) and (5) with the similarity transformations (6)

$$f' = 1, \quad f = S, \quad \theta = 1 - St \quad \text{at} \eta = 0 \quad (9)$$

$$f' \to 0, \quad \theta \to 0 \quad \text{as} \eta \to \infty \quad (10)$$

Where the prime denotes differentiation with respect to $\eta$ ,

$M = B_o \frac{\sqrt{L\sigma}}{\rho U_0}$ is the magnetic parameter, $S = \frac{v_0}{\sqrt{\frac{U_0 \nu}{2L}}} < 0)$ is the blowing parameter, $St = \frac{c}{b}$ is the stratification parameter and $\Pr = \frac{\mu c_p}{\kappa}$ is the Prandtl number, $Rd = \frac{4T_\infty^3 \sigma}{3kk^*}$ is the radiative parameter $N$ , is the exponentially stretching sheet parameter, and $k_1 = \frac{2\nu L}{k_0 U_0}$ is the permeability parameter. For $St > 0$ , gives a stably stratified environment, while $St = 0$ implies an unstratified environment.

Lai and Kulacki (1991) discussed the skin friction coefficient and the Nusselt number which are vital physical quantities in our problem. These quantities are defined as
Skin friction coefficient,

$$c_f = -\frac{U_0}{x\sqrt{2}} \left( \frac{\partial u}{\partial y} \right)_{y=0} = f''(0) \quad (11)$$

Nusselt number,

$$Nu = x \left( \frac{\partial T}{\partial y} \right)_{y=0} = -\theta'(0) \quad (12)$$

**2.2 Conversion of higher-order ODEs to first-order ODEs form**

In the solution technique, we obtain a system of first-order ordinary differential equations from the determined higher-order ordinary differential equations.
For

$$f''' - 2Nf'^2 + Nff'' - (k_1 + 2M^2 \sin^2 \alpha) f' = 0 \text{ and}$$

$$\theta'' + \frac{N \Pr}{\left(1 + \frac{4}{3} Rd\right)} \{ f\theta' - \theta f'\} - \frac{N \Pr St}{\left(1 + \frac{4}{3} Rd\right)} f' = 0$$

Let $u_1 = f$, $u_2 = f'$, $u_3 = f''$, $u_4 = \theta$, $u_5 = \theta'$ To obtain system below

$$u_1' = u_2$$
$$u_2' = u_3$$
$$u_3' = 2Nu_2^2 - Nu_1u_3 + \left(k_1 + 2M^2\sin^2\alpha\right)u_2$$
$$u_4' = u_5 \qquad (13)$$
$$u_5' = \frac{N\ \mathrm{Pr}}{\left(1+\frac{4}{3}Rd\right)}\left(u_4u_2 - u_1u_5\right) + \frac{N\ \mathrm{Pr}\ St}{\left(1+\frac{4}{3}Rd\right)}u_2$$

With boundary conditions

$$u_1 = S, \quad u_2 = 1, \quad u_3 = 0, \quad u_4 = 1 - St, \quad u_5 = 0 \quad at \quad \eta = 0 \qquad (14)$$

$$u_2 \to 0, \quad u_4 \to 0 \quad as \quad \eta \to \infty \qquad (15)$$

**2.3 Numerical solution**

To solve the system of equations above numerically, we use the collocation method. For this method to apply, the system of equations above is written in vector form as below

$$\vec{u}\,' = \vec{g}\left(\eta, \vec{u}, \vec{p}\right) \quad for\ 0 \le \eta < \infty \qquad (16)$$

Where $\vec{u} = \left(u_1, u_2, u_3, u_4, u_5\right)^T$ , $\vec{g} = \left(g_1, g_2, g_3, g_4, g_5\right)^T$ and $\vec{p}$ is a vector of unknown parameters. $\vec{g}$ Takes the values

$$g_1 = u_2$$
$$g_2 = u_3$$
$$g_3 = 2Nu_2^2 - Nu_1u_3 + \left(k_1 + 2M^2\sin^2\alpha\right)u_2$$
$$g_4 = u_5$$
$$g_5 = \frac{N\ \mathrm{Pr}}{\left(1+\frac{4}{3}Rd\right)}\left(u_4u_2 - u_1u_5\right) + \frac{N\ \mathrm{Pr}\ St}{\left(1+\frac{4}{3}Rd\right)}u_2$$

Equation (16) is solved subject to boundary conditions, see 14, 15

$$\vec{h}\left(\vec{u}(0), \vec{u}(\infty), \vec{p}\right) = 0 \qquad (17)$$

For simplicity, we suppress $\vec{p}$ in equation (16) to get an approximate solution $\vec{S}(\eta)$ to $\vec{u}(\eta)$, which is a continuous function that is a cubic polynomial on each subinterval $(\eta_n, \eta_{n+1})$ of a mesh $0 = \eta_0 < \eta_1 < \ldots\ldots\ldots\ldots < \eta_N = \infty$ . This approximate solution satisfies:

(a) The boundary conditions

$\vec{h} = \left(S(0), S(\infty)\right) = 0$ (18)(b) differential equations (collocates) at both ends and the midpoint of each of the following subinterval

$$\vec{S}\,'(\eta_n) = \vec{g}\left(\eta_n, \vec{S}(\eta_n)\right)$$
$$\vec{S}\,'\left(\left(\eta_n + \eta_{n+1}\right)/2\right) = \vec{g}\left(\left(\eta_n + \eta_{n+1}\right)/2, \vec{S}\left(\eta_n + \eta_{n+1}\right)/2\right)$$
$$\vec{S}\,'(\eta_{n+1}) = \vec{g}\left(\eta_{n+1}, \vec{S}(\eta_{n+1})\right)$$

These conditions give a system of nonlinear algebraic equations for the coefficients defining $\vec{S}(\eta)$, which is a cubic polynomial approximating the solution $\vec{u}(\eta)$ over the whole interval $[0, \infty)$

In collocation, these nonlinear equations are solved iteratively by linearization subject to the conditions

$$\left\|\vec{u}(\eta) - \vec{S}(\eta)\right\| \le Ch^4 \qquad (19)$$

Where $h$ the maximum of the step sizes $h_n = \eta_{n+1} - \eta_n$ for $n = 1,2,\ldots\ldots\ldots N$ and $C$ is a constant. For the initial guess in the collocation method, we note that the continuity of $\vec{S}(\eta)$ on $[0,\infty)$ and collocation at the ends of each subinterval imply that $\vec{S}(\eta)$ also has a continuous derivative on $[0,\infty)$. Therefore for an approximate $\vec{S}(\eta)$, a residue $\vec{r}(\eta)$ in the above system of ODEs is computed as below

$$\vec{r}(\eta) = \vec{S}(\eta) - \vec{g}\left(\eta, \vec{S}(\eta)\right) \quad (20)$$

Similarly, the residual in the boundary conditions are obtained from (20) above. If the residuals are uniformly small, then $\vec{S}(\eta)$ is the required approximation of the exact solution $\vec{u}(\eta)$. The idea behind this is to ensure that the residuals are minimized by making sure that the condition (19) is met at each point.

## 3. RESULTS AND DISCUSSION

The importance of this section is to analyze the effect of various physical parameters on the velocity and temperature profiles on the fluid flow. The results are presented graphically in figures 2-10 followed by a detailed discussion on the interpretation of the same for parameters such as, Exponential stretching $(N)$, Stratification $(St)$, Magnetic $(M)$, Radiative $(Rd)$, Angle of inclination $(\alpha)$, and Prandtl number $(\mathrm{Pr})$ which we chose to range between 4 and 6 for surfactants (Drag reducing agents). Also, various values for skin friction coefficient $f''(0)$ and Nusselt number $-\theta'(0)$ were obtained for each parameter and tabulated in table 1.

### 3.1: Effects of variation of magnetic parameter on velocity and temperature profiles

Fig.2 shows the effect of magnetic parameter $M$ on the velocity profile for the fluid flow when other parameters are kept constant. According to the referred figure, the velocity decreases as values of $M$ increase. This is because an increase in the magnetic field increases Lorentz's force. This offers more resistance to the motion of the fluid and thus the velocity of the fluid is reduced. In *fig.3* the temperature increases with an increase in magnetic parameter $M$ . This is because larger values of magnetic parameter correspond to an increase in Lorentz force which is a resistive force. This resistive force increases the thermal boundary layer which increases the temperature profile.

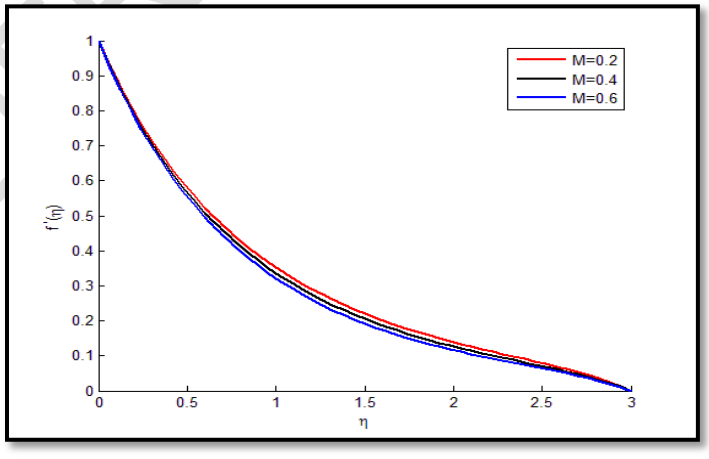


**Figure 2: Velocity profile for different values of magnetic parameter**

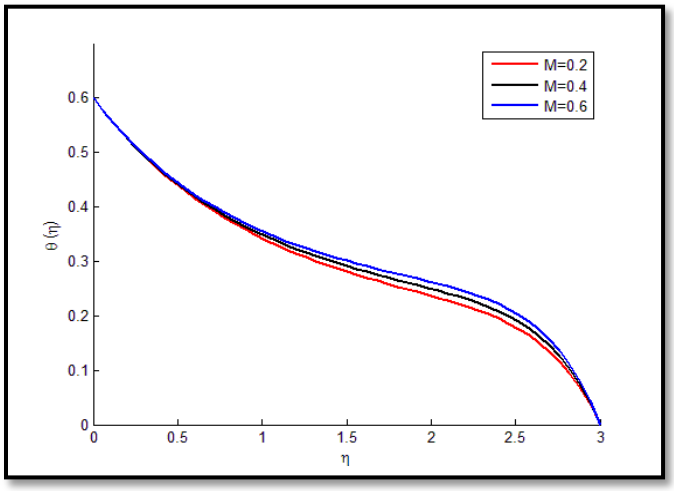


**Figure 3: Temperature profile for various values of magnetic parameter**

### 3.2: Effects of variation of the angle of inclination on velocity and temperature profiles

*Fig.4* represents the effect of the angle of inclination $\alpha$ on the velocity profile. From the figure, the velocity profile decreases with increasing value of angle of inclination $\alpha$. This can be attributed to the fact that an increase in the angle of inclination, increases the magnetic field effect on the fluid which in turn increases the Lorentz force resulting in the decreased velocity profile. According to the result obtained it is clear that maximum resistance is experienced by the fluid particles when the angle is $\frac{\pi}{2}$.

*Fig.5* shows the variation of the angle of inclination $\alpha$ on the temperature profile. According to the figure referred, the temperature profile is higher for larger values of angle $\alpha$. This is because higher values of angle $\alpha$ correspond to a larger magnetic field which opposes motion. This makes the thermal boundary layer increase, therefore, increasing the temperature profile

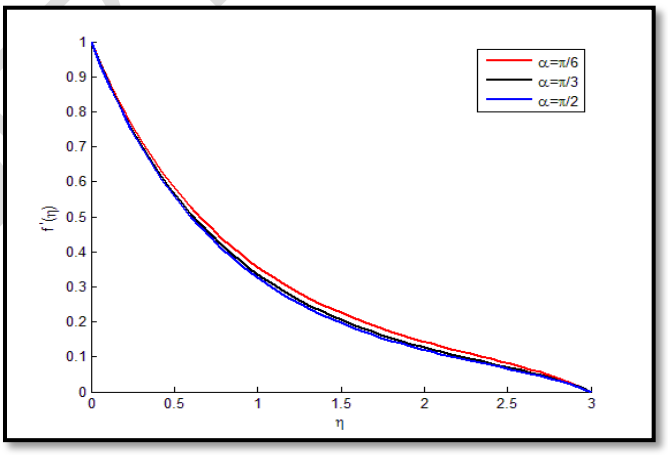


**Figure 4: Velocity profile for different values of angle of inclination**

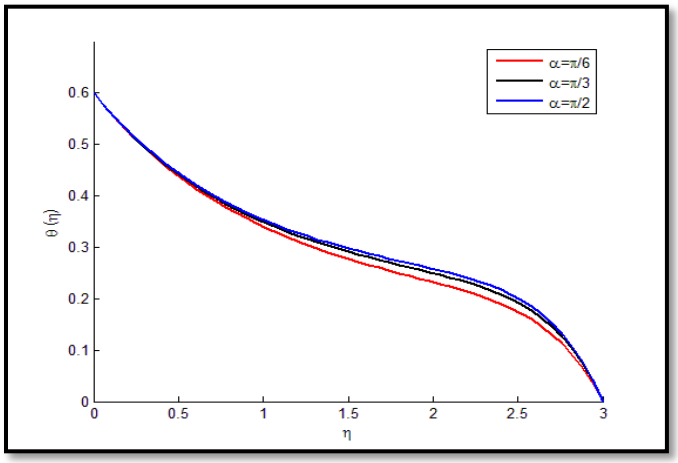


**Figure 5: Temperature profile for different values of angle of inclination**

### 3.3:Effects of stretching parameter on velocity and temperature profiles

*Fig.6* Shows the effect of exponential stretching parameter $N$ on the velocity profile $f'(\eta)$. It is noted that the fluid velocity increases with an increase in $N$. This is because the stretching of the sheet wall reduces the momentum boundary layer which leads to the reduction of the viscosity which in turn makes the fluid flow faster.

*Fig.7* depicts the effect of exponential parameter $N$ on the temperature profile. It is noted that the temperature decreases with increasing $N$ because the thermal boundary layer thickness decreases with increasing $N$. This makes the wall temperature decrease throughout the boundary layer.

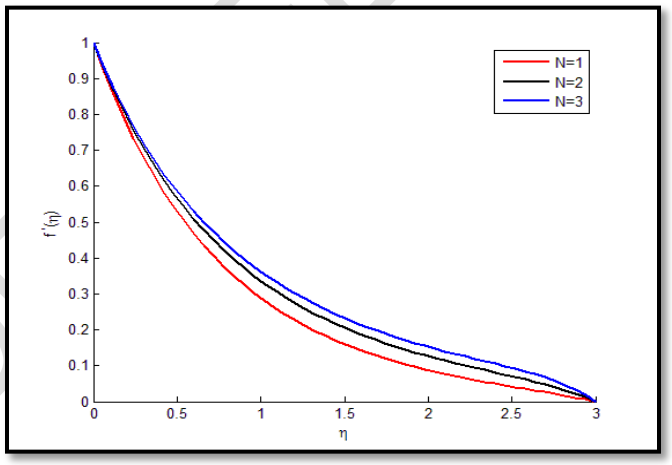


**Figure 6: Velocity profile for different values of the exponential stretching parameter**

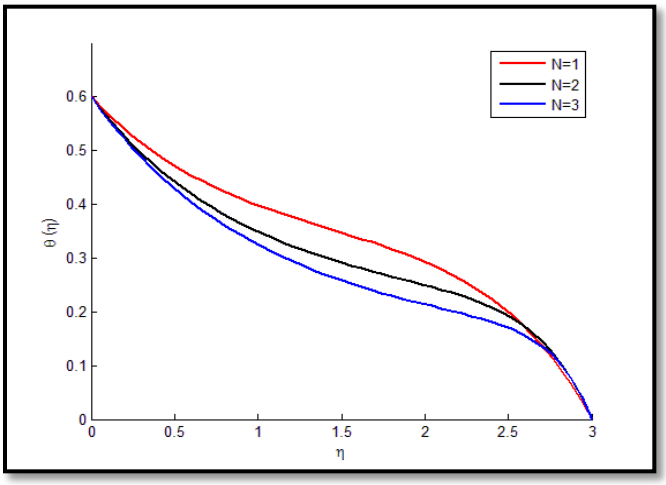


**Figure 7: Temperature profile for different values of the exponential stretching parameter**

### 3.4:Effects of stratification parameter on velocity and temperature profiles

Fig.8 shows the temperature profile $\theta'(\eta)$ for various values of the stratified parameter. It is noted that the temperature decreases as the stratified parameter increases. This is because an increase in stratification parameter $St$ means a decrease in surface temperature. This makes the thermal boundary layer thickness decrease leading to less heat diffusion thus decreasing the temperature profile. On velocity profile, variation in stratification parameter has no observable effect.

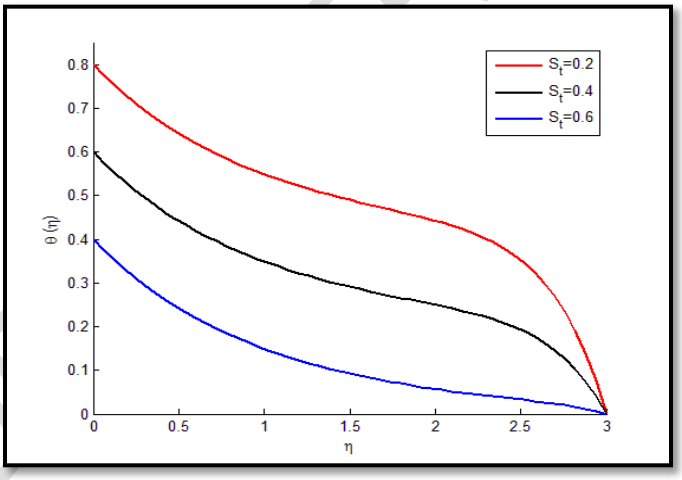


**Figure 8: Temperature profile for different values of stratification parameter**

### 3.5: Effects of Prandtl number on velocity and temperature profiles

Prandtl number $\Pr$ is the ratio of momentum diffusivity to thermal diffusivity. In heat transfer, it controls the relative thickness of the momentum and thermal boundary layer. In *fig.9*, the temperature decreases with the increase in the Prandtl number for some length $\eta < 2.25$ . This is because an increase in the Prandtl number makes the thermal boundary layer decrease. This makes heat diffusion to be slow and therefore thermal conductivity becomes small resulting in a decrease in the temperature profile. Beyond $\eta = 2.25$ there is an insignificant rise in temperature. For the velocity profile, the Prandtl number has no effect.

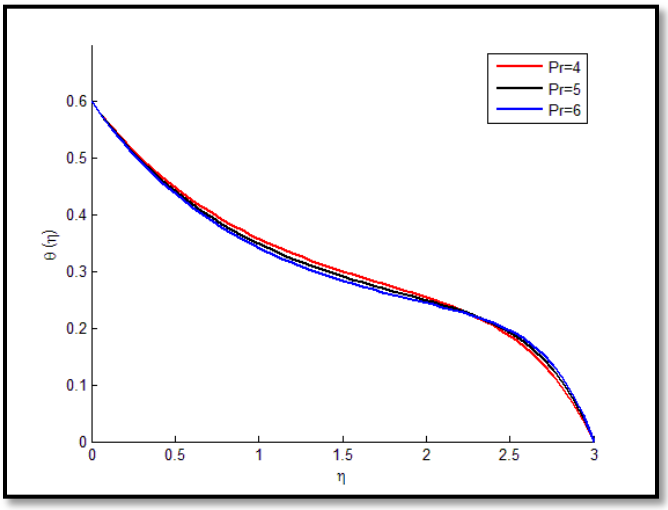


**Figure 9: Temperature profile for different values of Prandtl number**

### 3.6: Effects of Radiative parameter on velocity and temperature profiles

Fig.10 depicts the effect of the radiation parameter $Rd$ on the temperature profile. It is noted that as the $Rd$ increases the temperature increases. This is due to the enhancement of thermal boundary layer thickness which provides more heat to the fluid and this results in an enhancement in the temperature profile. Beyond $\eta = 2.25$ higher temperature is not maintained, therefore it drops drastically. No effect of radiation on the velocity profile.

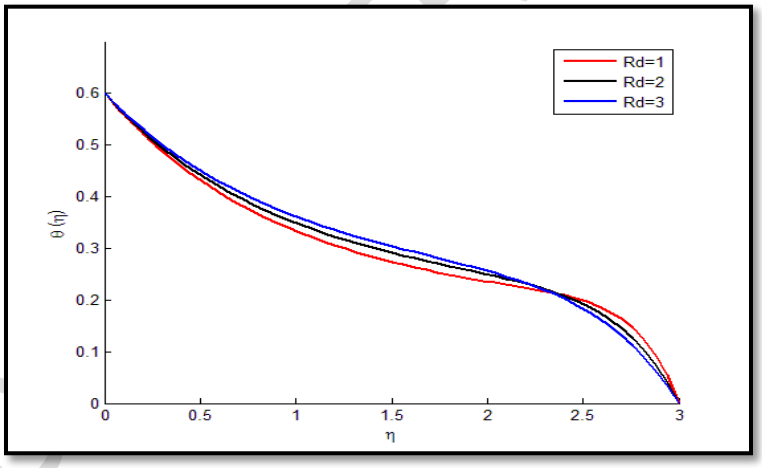


**Figure 10: Temperature profile for different values of Radiative profile**

### 3.7: Effects of parameters variation on the skin friction $C_f$ and Nusselt number $Nu$ .

Table 1 shows the effect of magnetic $M$ , angle of inclination $\alpha$ , permeability $k_1$ , radiation $Rd$ , injection $S$ , Prandtl number $\Pr$ and the exponential stretching $N$ parameters on skin friction coefficient $C_f$ and Nusselt number $Nu$ . It is noted that the skin friction and Nusselt number are associated with fluid velocity and heat transfer rate respectively. From the table, it is observed that increase in permeability parameter $k_1$ results in a reduction in skin friction coefficient and decrease in Nusselt number. Permeability being the measure of the ability of a porous material to allow the fluid to pass through it, the increase in this parameter reduces the shear stress, which is the measure of the force of friction. This reduced shear stress results in a reduction in skin friction. For Nusselt number, permeability results in a decrease in viscosity. Now that the

fluid injection is constant, the overall fluid temperature will increase to a maximum point thus resulting in less heat transfer.

We also observe that the exponential stretching parameter results in an increase in skin friction and an increase in Nusselt number. This is attributed to the fact that stretching of the wall surface results in a decrease in velocity boundary layer thus increase in fluid velocity. This in turn increases the contact of fluid particles with the surface, thus increasing the skin friction. For the Nusselt number, an increase in stretching parameter reduces the momentum boundary layer which makes more fluid particles to be in contact with the surface of the sheet. This enhances heat transfer in the fluid through convection, thus increasing the Nusselt number.

Injection (blowing) through the wall results in an increase in skin friction and a decrease in Nusselt number. An increase in Skin friction is due to the pushing of the heated fluid away from the wall, resulting in less viscosity on the wall. For Nusselt number, injection increases the overall fluid temperature to a maximum point. This reduces the heat transfer rate, hence decrease in Nusselt number

When the strength of the magnetic field and angle of inclination increases, it is noted that the Skin friction coefficient decreases, and the Nusselt number insignificantly decreases. The physical explanation given is that increase in magnetic field strength and angle of inclination makes the Lorentz force large thus reducing the fluid motion. This increases the no-slip effect thus decreasing skin friction. For Nusselt number, the decrease is due to less transfer of the heat from one point to another in the flow field as a result of increased overall fluid temperature.

Parameters such as $St$ , $Rd$ , and $\Pr$ do not affect Skin friction coefficient even if they are varied. Also on Nusselt number, $St$ has no effect. But an increase in $Rd$ and $\Pr$ makes the Nusselt number decrease and increase respectively. This is because higher $\Pr$ fluid has a relatively lower thermal conductivity which reduces conduction and thereby increasing heat transfer rate at the surface. Larger values of $Rd$ increase thickness of the thermal boundary layer resulting in a decrease in heat transfer.

**Table 1: Values of Skin friction coefficient $f''(0)$ and Nusselt number $-\theta'(0)$ for various parameters**

| $N$ | $St$ | $\alpha$ | $M$ | $Rd$ | $\Pr$ | $f''(0)$ | $-\theta'(0)$ |
|---|---|---|---|---|---|---|---|
| 2 | 0.4 | $\pi/3$ | 0.4 | 2 | 5 | -0.9699 | 0.3975 |
| 2 | | | | | | -1.2321 | 0.3728 |
| 1 | | | | | | -1.2066 | 0.3174 |
| 2 | | | | | | -1.1051 | 0.3846 |
| 3 | | | | | | -1.0548 | 0.4119 |
| 2 | | | | | | -1.4839 | 0.5797 |
| | 0.4 | | | | | -0.8616 | 0.2846 |
| | 0.2 | | | | | -1.1051 | 0.3846 |
| | 0.4 | | | | | -1.1051 | 0.3846 |
| | 0.6 | $\pi/3$ | | | | -1.1051 | 0.3846 |
| | 0.4 | $\pi/6$ | | | | -1.0520 | 0.3897 |
| | | $\pi/3$ | | | | -1.1051 | 0.3846 |
| | | $\pi/2$ | 0.4 | | | -1.1311 | 0.3822 |
| | | $\pi/3$ | 0.2 | | | -1.0654 | 0.3884 |
| | | | 0.4 | | | -1.1051 | 0.3846 |
| | | | 0.6 | 2 | | -1.1440 | 0.3810 |
| | | | 0.4 | 1 | | -1.1051 | 0.4100 |

| | | | | | | | |
|---|---|---|---|---|---|---|---|
| | | | | 2 | | -1.1051 | 0.3846 |
| | | | | 3 | 5 | -1.1051 | 0.3627 |
| | | | | 2 | 4 | -1.1051 | 0.3692 |
| | | | | | 5 | -1.1051 | 0.3846 |
| | | | | | 6 | -1.1051 | 0.3958 |

## 4. Conclusion

The boundary layer flow of a viscous incompressible fluid over an exponentially stretching sheet with an inclined magnetic field in the presence of thermal radiation was studied. The governing continuity, momentum, and energy equations were obtained by use of suitable similarity transformation variables. The higher-order non-linear differential equations obtained were reduced to a system of first-order ordinary differential equations. The numerical solutions were computed by the collocation method. The numerical results for the governing parameters were presented graphically. Also, various numerical values for skin friction and Nusselt number were obtained for each parameter. Some of the main conclusions made are:

i. Velocity profile decreases with increase in strength of magnetic field and angle of inclination
ii. There is an increase in temperature profile when the strength of the magnetic field, angle of inclination of the material increases. It also increases when the radiative Property of the material increases.
iii. Temperature profile decreases with an increase in exponential stretching of the material, stratification of the material, and Prandtl number.
iv. There is a decrease in skin friction when the angle of inclination increases but increases with an increase in exponential stretching of the material.
v. Nusselt number increases with an increase in exponential stretching, and Prandtl number but decreases with an increase in the magnetic field, angle of inclination, and radiative property of the material.

**References**


[1] I. Ullah, S. Shafie, and I. Khan, “Effects of slip condition and Newtonian heating on MHD flow of Casson fluid over a nonlinearly stretching sheet saturated in a porous medium,” *J. King Saud Univ. - Sci.*, vol. 29, no. 2, pp. 250–259, Apr. 2017, doi: 10.1016/J.JKSUS.2016.05.003.

[2] K. Sharma and S. Gupta, “Analytical study of MHD boundary layer flow and heat transfer towards a porous exponentially stretching sheet in presence of thermal radiation,” *Int. J. Adv. Appl. Math. Mech.*, vol. 4, no. 1, pp. 2347–2529, 2016.

[3] B. K. Jha and B. Aina, “Effect of induced magnetic field on MHD mixed convection flow in vertical microchannel,” *Int. J. Appl. Mech. Eng.*, vol. 22, no. 3, pp. 567–582, Aug. 2017, doi: 10.1515/IJAME-2017-0036.

[4] A. S. Idowu and B. O. Falodun, “Influence of Magnetic Field and Thermal Radiation on Steady Free Convective Flow in a Porous Medium,” *Niger. J. Technol. Dev.*, vol. 15, no. 3, p. 84, Aug. 2018, doi: 10.4314/njtd.v15i3.3.

[5] A. K. Pandey and M. Kumar, “Natural convection and thermal radiation influence on nanofluid flow over a stretching cylinder in a porous medium with viscous dissipation,” *Alexandria Eng. J.*, vol. 56, no. 1, pp. 55–62, Mar. 2017, doi: 10.1016/j.aej.2016.08.035.

[6] N. A. H. Haroun, S. Mondal, and P. Sibanda, “Effects of Thermal Radiation on Mixed Convection in a MHD Nanofluid Flow over a Stretching Sheet Using a Spectral Relaxation Method,” *Int. J. Math. Comput. Sci.*, vol. 11, no. 2, pp. 52–61, 2017.

[7] S. R. R. Chandra Babu, S. Venkateswarlu, and K. J. Lakshmi, “Effect of Variable Viscosity and Thermal Conductivity on Heat and Mass Transfer Flow of Nanofluid over a Vertical Cone with Chemical Reaction,” *Int. J. Appl. Eng. Res.*, vol. 13, pp. 13989–14002, 2018.

[8] B. K. Jha, B. Y. Isah, and I. J. Uwanta, “Combined effect of suction/injection on MHD free-convection flow in a vertical channel with thermal radiation,” *Ain Shams Eng. J.*, vol. 9, no. 4, pp. 1069–1088, Dec. 2018, doi: 10.1016/j.asej.2016.06.001.

[9] S. Chaudhary, K. M. Kanika, and M. K. Choudhary, “Newtonian heating and convective boundary condition on MHD stagnation point flow past a stretching sheet with viscous dissipation and Joule heating,” 2018.

[10] M. Javanmard, M. H. Taheri, and S. M. Ebrahimi, “Heat transfer of third-grade fluid flow in a pipe under an externally applied magnetic field with convection on wall,” *Appl. Rheol.*, vol. 28, no. 5, pp. 1–11, 2018, doi: 10.3933/ApplRheol-28-56023.

[11] D. Khan, A. Khan, I. Khan, F. Ali, F. Karim, and I. Tlili, “Effects of Relative Magnetic Field , Chemical Reaction , Heat Generation and Newtonian Heating on Convection Flow of Casson Fluid over a Moving Vertical Plate Embedded in a Porous Medium,” *Sci. Rep.*, vol. 9, no. 400, pp. 1–18, 2019, doi: 10.1038/s41598-018-36243-0.

[12] S. Jagadha and P. Amrutha, “MHD Boundary Layer Flow of Darcy-Forchheimer Mixed Convection in a Nanofluid Saturated Porous Media with Viscous Dissipation,” *Appl. Appl. Math.*, vol. 4, no. 4, pp. 117–134, 2019.

[13] W. Ibrahim and A. Tulu, “Magnetohydrodynamic (MHD) Boundary Layer Flow Past a Wedge with Heat Transfer and Viscous Effects of Nanofluid Embedded in Porous Media,” *Math. Probl. Eng.*, vol. 2019, no. 4507852, pp. 1–12, 2019, doi: 10.1155/2019/4507852.

[14] A. O.A., A. L.O., A. S.F., and O. A.W., “Effect of Magnetic Fields on the Boundary Layer Flow of Heat Transfer with Variable Viscosity in the Presence of Thermal Radiation,” *Int. J. Sci. Res. Publ.*, vol. 9, no. 5, p. p8904, 2019, doi: 10.29322/ijsrp.9.05.2019.p8904.

[15] S. H. M. Yasin, M. K. A. Mohamed, Z. Ismail, B. Widodo, and M. Z. Salleh, “MHD Flow and Heat Transfer of Ferrofluid on Stagnation Point along Flat Plate with Convective Boundary Condition and Thermal Radiation Effect,” *J. Phys. Conf. Ser.*, vol. 1366, no. 1, 2019, doi: 10.1088/1742-6596/1366/1/012008.

[16] K. Gangadhar, D. Vijaya Kumar, M. Venkata Subba Rao, T. Kannan, and G. Sakthivel, “Effects of Newtonian heating on the boundary layer flow of non-Newtonian magnetohydrodynamic nanofluid over a stretched plate using spectral relaxation method,” *Int. J. Ambient Energy*, 2019, doi: 10.1080/01430750.2019.1694585.

[17] M. H. Taheri, “The influence of magnetic field on the fluid flow in the entrance region of channels: analytical/numerical solution,” *SN Appl. Sci.*, vol. 1, no. 10, Oct. 2019, doi: 10.1007/S42452-019-1244-3.

[18] D. Kumar, A. K. Singh, and D. Kumar, “Influence of heat source/sink on MHD flow between vertical alternate conducting walls with Hall effect,” *Phys. A Stat. Mech. its Appl.*, vol. 544, Apr. 2020, doi: 10.1016/J.PHYSA.2019.123562.

[19] B. K. Jha and G. Samaila, “Thermal radiation effect on boundary layer over a flat plate having convective surface boundary condition,” *SN Appl. Sci. 2020 23*, vol. 2, no. 3, pp. 1–8, Feb. 2020, doi: 10.1007/S42452-020-2167-8.

[20] K. Gangadhar, D. Vijayakumar, A. J. Chamkha, T. Kannan, and G. Sakthivel, “Effects of Newtonian heating and thermal radiation on micropolar ferrofluid flow past a stretching surface: Spectral quasi-linearization method,” *Heat Transf. - Asian Res.*, vol. 49, no. 2, pp. 838–857, 2019, doi: 10.1002/HTJ.21641.

[21] A. A. Afify and N. S. Elgazery, “Impacts of Newtonian heating, variable fluid properties and Cattaneo–Christov model on MHD stagnation point flow of Walters’ B fluid induced by stretching surface,” *Int. J. Mod. Phys. C*, vol. 31, no. 9, p. 2050125, Aug. 2020, doi: 10.1142/S0129183120501259.